



Contents lists available at ScienceDirect

Nuclear Instruments and Methods in Physics Research A

journal homepage: www.elsevier.com/locate/nima

Dynamics of electromagnetic two-stream interaction processes during longitudinal and transverse compression of an intense ion beam pulse propagating through background plasma

Edward A. Startsev*, Ronald C. Davidson

Plasma Physics Laboratory, Princeton University, Princeton, NJ 08543, USA

ARTICLE INFO

Available online 21 March 2009

Keywords:

Two-stream instability
Dynamic stabilization
Charged-particle beams

ABSTRACT

To achieve maximum energy density, an intense ion beam must be compressed radially and longitudinally while its space-charge is neutralized by background plasma. An ion beam propagating through background plasma may be subject to the electrostatic two-stream instability and the electromagnetic Weibel instability. The electrostatic two-stream instability may lead to longitudinal bunching of the beam pulse, and eventual longitudinal beam heating. Consequently, this could degrade the longitudinal compression of the beam pulse. Similarly, the electromagnetic Weibel instability may cause transverse filamentation of the beam, which may degrade transverse compression. In this paper, we use an eikonal (Wentzel–Kramer–Brillouin, WKB) approach to analyze the space–time development of the two-stream and Weibel instabilities during transverse and longitudinal compression of an intense heavy ion beam pulse propagating through neutralizing background plasma.

© 2009 Elsevier B.V. All rights reserved.

1. Introduction

For inertial fusion energy and high energy density physics applications, the energy of an intense laser or particle beam has to be delivered and deposited in the target within a small volume during a short period of time. In the heavy ion approach, the energy is delivered by intense heavy ion beams with very low transverse emittance [1]. After the acceleration phase, the ion beam density must be compressed transversely and longitudinally by factors of 10^4 or more to access the regimes relevant to ion-beam-driven high energy density physics and fusion. Accessing such highly compressed beam conditions is greatly facilitated by the use of dense, large-volume background plasma to provide charge and current neutralization of the ion beam pulse during the longitudinal and transverse compression phases [2–7]. Therefore, it is extremely important to understand how collective beam–plasma instabilities are driven by the beam, and what effect the radial and longitudinal focusing has on the space–time development of these instabilities.

Previous studies of beam–plasma instabilities have concentrated on solving a linearized system of integro-differential Vlasov–Maxwell equations for an intense ion beam converging in a neutralizing background plasma [2,8–10]. The equations are

often too complex to be analyzed in detail. Even if analytic solutions can be found, useful expressions for instability growth rates/gains can be obtained only by assuming that the beam flow profiles evolve more slowly than the unstable perturbations in space and time. In this case, the asymptotic formulas for the instability gains can be obtained from the formal solutions of the equations. In this paper, it is proposed to use the geometrical optics eikonal (Wentzel–Kramer–Brillouin, WKB) method [11,12] from the beginning of the analysis, in order to avoid dealing with the complex linearized system of integro-differential Vlasov–Maxwell equations. In this approach, a slow space–time change of profiles is assumed from the onset, which simplifies the analysis, and allows the asymptotic solutions to be obtained with much less effort.

This paper is organized as follows. In Sections 2 and 3, we discuss how the transverse focusing and longitudinal focusing of intense heavy ion beams are achieved, and determine the leading-order unperturbed focusing profiles obtained by passing the beam through a neutralizing background plasma. In Section 4, we introduce the geometrical optics eikonal (WKB) method for solving the unstable beam–plasma dynamics. In Section 5, we briefly discuss the ray equations for the waves. In Section 6, we analyze the electrostatic two-stream instability for a transversely (Section 6.1) and longitudinally (Section 6.2) converging heavy ion beam using the eikonal method. The electromagnetic filamentation (Weibel) instability is examined in Section 7. Finally, the main results are summarized in Section 8.

* Corresponding author.

E-mail address: estarts@pppl.gov (E.A. Startsev).

2. Transverse focusing of a heavy ion beam

Transverse focusing can be achieved by passing the ion beam through a solenoidal magnet. When beam enters the solenoid, it begins to rotate. The angular velocity of rotation can be obtained from conservation of canonical angular momentum, which gives

$$v_\theta = \frac{qA_\theta}{m_b c} = r \frac{qB_\parallel}{2m_b c} = \frac{r\omega_{cb}}{2}. \quad (1)$$

Here, $\omega_{cb} = qB_\parallel/m_b c$ is the beam ion cyclotron frequency. If the beam is charge-neutralized by the background plasma, or if the beam density is low enough that $\omega_{pb} \ll \omega_{cb}$, where $\omega_{pb}^2 = 4\pi q^2 n_b/m_b$ is the beam plasma frequency-squared, then the radial acceleration is due to the centrifugal force and the Lorentz force. This gives [1]

$$\frac{dv_r}{dt} = \frac{v_\theta^2}{r} - \frac{qB_\parallel}{mc} v_\theta = -r \frac{\omega_{cb}^2}{4}. \quad (2)$$

It follows from Eq. (2) that a thin solenoid with length $d \ll v_b/\omega_{cb}$ behaves as an ideal lens (linear optics element). After passing through the solenoid, the beam acquires a linear radial velocity profile, $v_\perp \sim -x_\perp$. If after the solenoid the beam propagates through a neutralizing background plasma along the x -direction, then the beam flow velocity v_\perp, v_\parallel , the beam density n_b , and the transverse beam temperature $v_{th\perp}$ change with distance according to Ref. [8]

$$v_\perp = -\frac{x_\perp v_b}{X_f - x}, \quad v_\parallel = v_b, \quad n_b = \frac{n_{b0}}{(1 - x/X_f)^2} \quad (3)$$

$$v_{th\perp} = \frac{v_{th0}}{(1 - x/X_f)}. \quad (4)$$

Here X_f is the focal length for the solenoidal magnetic lens.

3. Longitudinal focusing of a heavy ion beam

Longitudinal focusing of a heavy ion beam is achieved by passing the beam through an induction core with a time-dependent voltage, designed to impose a longitudinal velocity tilt which is a linear function along the beam, i.e., $v_\parallel - v_b \sim -x$ [2–4,13–17]. If after exiting the induction core, the beam space-charge is fully neutralized by the background plasma, the beam density and velocity change with time and distance according to Refs. [2,10]

$$n_b(t) = \frac{n_{b0} T_f}{T_f - t} \quad (4)$$

$$v_\parallel(t, x) = \frac{v_b T_f - x}{T_f - t} \quad (5)$$

where $x = 0$ corresponds to the beam entry positions into the plasma and $T_f = X_f/v_b$ is the time when the beam is completely focused longitudinally at $x = X_f$.

Fig. 1 illustrates the longitudinal phase space (x, v_\parallel) of the beam ions at different times during the longitudinal compression.

4. Eikonal (WKB) method

The compressing motion of a heavy ion beam propagating through a neutralizing background plasma described by Eqs. (3)–(5) can be unstable to electrostatic and electromagnetic perturbations. To describe the unstable linear dynamics of the perturbations, the Vlasov–Maxwell equations describing the beam and plasma components are linearized around the field-free solutions given by Eqs. (3)–(5). The resulting integro-differential equations are often too complicated to analyze in

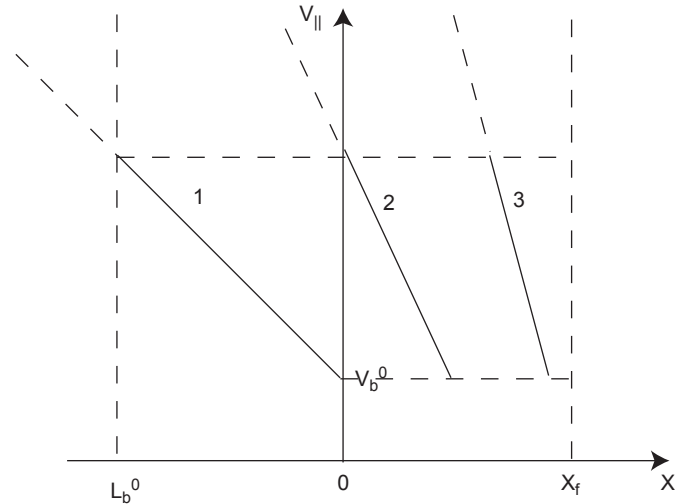


Fig. 1. Longitudinal phase space (x, v_\parallel) for the beam ions at different times during the longitudinal compression.

detail. A significant simplification can be achieved if the equilibrium profiles change in space and time much more slowly than the perturbations. In this case, the eikonal, geometrical optics, or Wentzel–Kramér–Brillouin method [11] can be used to obtain the desired solution. In this approach, the solution of the linearized equations can be represented in the eikonal form

$$a \sim \exp(iS). \quad (6)$$

After substituting this form of the solution into the linearized equations, and using $|S'| \ll |S|^2$ (WKB approximation), we obtain the equation for the eikonal S , i.e.,

$$D(\mathbf{k}, \omega) = 0 \quad (7)$$

where $\mathbf{k} = \partial S / \partial \mathbf{x}$ and $\omega = -\partial S / \partial t$. The dispersion relation $D(\mathbf{k}, \omega) = 0$ becomes a Hamilton–Jacobi equation for the waves. The approximation $|S'| \ll |S|^2$ implies that the solution is almost a plane wave, locally. This approach works well for both cold plasmas described by macroscopic fluid–Maxwell equations, and for warm plasmas described by the Vlasov–Maxwell equations.

To determine the solution to Eq. (7), we can use the methods developed in solving the Hamilton–Jacobi equation in classical mechanics. We are interested in the so-called *full integral* solution, where the eikonal S is a function of the number of constants of the motion, which is one less than the number of independent variables (\mathbf{x}, t) . Here, we are not interested in additive constants, since they can be removed by renormalizing the amplitude a .

After the *full integral* solution is found, the amplitude is obtained as a linear combination (integral) over all sets of parameters \mathbf{q} (analog of the Fourier integral)

$$a = \int d\mathbf{q} a(\mathbf{q}) \exp[iS(\mathbf{x}, t, \mathbf{q})] \quad (8)$$

where $a(\mathbf{q})$ is related to boundary conditions, or the initial value of a .

The asymptotic behavior of the solution a can be found by evaluating the integral in Eq. (8) using the stationary-phase method. The asymptotic form of the solution can then be expressed as

$$a \sim \exp[iS(\mathbf{x}, t, \mathbf{q}_{ext})] \quad (9)$$

where \mathbf{q}_{ext} is determined from

$$\frac{\partial S(\mathbf{x}, t, \mathbf{q}_{ext})}{\partial \mathbf{q}_{ext}} = 0. \quad (10)$$

As an example, consider the case when there is no space–time dependence in any plasma parameter. In this case, the independent variables are called *cyclic*, and the *full integral* solution of Hamilton–Jacobi equation can be expressed as

$$S = -\omega t + \mathbf{k} \cdot \mathbf{x} \quad (11)$$

where the frequency ω and wavenumber \mathbf{k} are constants of the motion and are related by the dispersion relation $D(\omega, \mathbf{k}) = 0$. The amplitude can be expressed as

$$a = \int d\mathbf{k} a(\mathbf{k}) \exp\{i[-\omega(\mathbf{k})t + \mathbf{k} \cdot \mathbf{x}]\} \quad (12)$$

which is the familiar Fourier representation of the solution of the Vlasov–Maxwell equations.

Applications of the method described above are illustrated by several examples presented in Sections 6 and 7.

5. Equation of motion for the waves

Instead of solving the Hamilton–Jacobi Eq. (7), we can use Eq. (7) to derive the ray equations for the waves, similar to Hamilton's equations in classical mechanics. By taking the partial time ($\partial/\partial t$) and space ($\partial/\partial \mathbf{x}$) derivatives of the Hamilton–Jacobi equation $D(\omega, \mathbf{k}) = 0$, we obtain

$$\begin{aligned} \frac{\partial \mathbf{k}}{\partial t} + \left(\mathbf{v}_g \cdot \frac{\partial}{\partial \mathbf{x}} \right) \mathbf{k} &\equiv \frac{d\mathbf{k}}{dt} = \frac{\partial D/\partial \mathbf{x}}{\partial D/\partial \omega}, \\ \frac{\partial \omega}{\partial t} + \left(\mathbf{v}_g \cdot \frac{\partial \omega}{\partial \mathbf{x}} \right) &\equiv \frac{d\omega}{dt} = -\frac{\partial D/\partial t}{\partial D/\partial \omega}. \end{aligned} \quad (13)$$

Here, the group velocity is given by

$$\mathbf{v}_g \equiv -\frac{\partial D/\partial \mathbf{k}}{\partial D/\partial \omega}. \quad (14)$$

This method is often useful if one wants to analyze the problem qualitatively. If one is interested in detailed quantitative solutions to the equations, this method is unnecessary, because it requires solving a system of second-order equations to find the ray trajectories $(\omega(t), \mathbf{k}(t))$, and then integrating to obtain the eikonal function S using the definitions $\mathbf{k} = \partial S/\partial \mathbf{x}$ and $\omega = -\partial S/\partial t$.

6. Electrostatic two-stream instability between the beam ions and plasma electrons

As a first illustration of the eikonal method, we consider the two-stream instability between the cold beam ions and the cold neutralizing plasma electrons. In this case, the dielectric function $D(\omega, \mathbf{k})$ is defined by

$$D = 1 - \frac{\omega_{pe}^2}{\omega^2} - \frac{\omega_{pb}^2(t, \mathbf{x})}{[\omega - \mathbf{k} \cdot \mathbf{v}_b(t, \mathbf{x})]^2}. \quad (15)$$

Here, $\omega_{pe}^2 = 4\pi e^2 n_0/m_e$ is the electron plasma frequency-squared, n_0 is the background plasma density, and $-e$ and m_e are electron charge and mass, respectively.

6.1. Two-stream instability during transverse compression

During transverse compression, the beam density and beam velocity change according to Eq. (3). By changing variables according to $S = S[t - x/v_b, 1/(1 - x/X_f), x_\perp/(1 - x/X_f)] = S(\tau, u, y)$, the Hamilton–Jacobi equation can be expressed as

$$1 = \frac{\omega_{pe}^2}{(\partial_\tau S)^2} + \frac{\omega_{pb0}^2 X_f^2}{[v_b u \partial_u S]^2} \quad (16)$$

where $\partial_\tau S = \partial S/\partial \tau$ and $\partial_u S = \partial S/\partial u$. Since τ and y are cyclic, the *full integral* for S can be expressed as

$$S = -\omega \tau + k_0 y \pm \left(\frac{\omega_{pb0} X_f}{v_b} \right) \frac{\ln u}{\sqrt{1 - \frac{\omega_{pe}^2}{\omega^2}}} \quad (17)$$

where ω and k_0 are constants. This expression is the same as that for the non-convergent case [18] if one makes the replacement $x \rightarrow X_f \ln u$. The asymptotic expression is found by extremizing S with respect to ω , which gives

$$S = -\omega_{pe} \tau + k_0 y + \frac{(1 - i\sqrt{3})3}{4} \left(\frac{\omega_{pb0} X_f \ln u}{v_b} \right)^{2/3} (\omega_{pe} \tau)^{1/3} \quad (18)$$

where the perturbations grow as $a \sim \exp(-\text{Im} S)$. The expression in Eq. (18) is valid for $\tau/T_f \gg (\omega_{pb}/\omega_{pe}) \ln u$. This expression was originally obtained in Ref. [9] by solving the system of linearized beam-plasma fluid and Poisson equations. As can be seen from Eq. (18), the instability growth is much faster for the case of a converging beam.

6.2. Two-stream instability during longitudinal compression

For longitudinal beam compression, the beam density and beam flow velocity vary according to Eqs. (4)–(5). The space–time development of the instability in this case has been analyzed in Ref. [2] by solving the system of linearized beam–plasma fluid and Poisson equations, and in Refs. [2,10] by analyzing the ray equations.

By changing variables according to $S = S(t/T_f - x/X_f, x/X_f) = S(\bar{\tau}, X)$, the Hamilton–Jacobi equation can be expressed as

$$1 = \frac{\beta^2}{(\partial_{\bar{\tau}} S)^2} + \frac{\alpha^2(1 - X - \bar{\tau})}{[(1 - X)\partial_X S - \bar{\tau}\partial_{\bar{\tau}} S]^2} \quad (19)$$

where $\beta = \omega_{pe} T_f$ and $\alpha = \omega_{pb0} T_f$. In the region where $(1 - X)|\partial_X S| \ll \bar{\tau}|\partial_{\bar{\tau}} S|$ the solution to Eq. (19) has the form

$$S = \beta \bar{\tau} - \frac{\alpha^2}{2\beta} \left[\frac{1 - X}{\bar{\tau}} + \ln \bar{\tau} \right] + \bar{S}(X) \quad (20)$$

which is valid for $\bar{\tau} \gg \alpha/\beta\sqrt{1 - X}$.

To determine $\bar{S}(X)$, we first obtain a solution valid in the region $\bar{\tau} \ll (1 - X)$, and then take the limit $(1 - X) \gg \bar{\tau} \gg \alpha/\beta\sqrt{1 - X}$. The region where $\bar{\tau} \approx (1 - X)$ corresponds to the time when the beam is fully compressed at $t \approx T_f$.

In the region $\bar{\tau} \ll (1 - X)$, we obtain $(1 - X - \bar{\tau}) \approx (1 - X)$, and Eq. (19) can be expressed as

$$1 = \frac{\beta^2}{(\partial_{\bar{\tau}} S)^2} + \frac{\alpha^2(1 - X)}{[(1 - X)\partial_X S - \bar{\tau}\partial_{\bar{\tau}} S]^2}. \quad (21)$$

By changing variables according to $S = S(\bar{\tau}/(1 - X), X) = S(T, X)$, Eq. (21) becomes

$$1 = \frac{\beta^2(1 - X)^2}{(\partial_T S)^2} + \frac{\alpha^2}{(1 - X)(\partial_X S)^2}. \quad (22)$$

Since in Eq. (22) T is cyclic, we look for a solution of the form $S = q\beta T + Q(X, q)$, with $q = \text{const}$. Substituting the solution of this form into Eq. (22) and integrating, we obtain the function $Q(X, q)$ given by

$$Q(X, q) = \pm 2\alpha q \int_1^{1/\sqrt{1-X}} \frac{dz}{\sqrt{z^4 q^2 - 1}}. \quad (23)$$

Therefore, in the region $\bar{\tau} \ll 1 - X$, the amplitude has the form

$$a(\bar{\tau}, X) = (1 - X) \int ds A[s(1 - X)] \exp[iS(\bar{\tau}, X, s)] \quad (24)$$

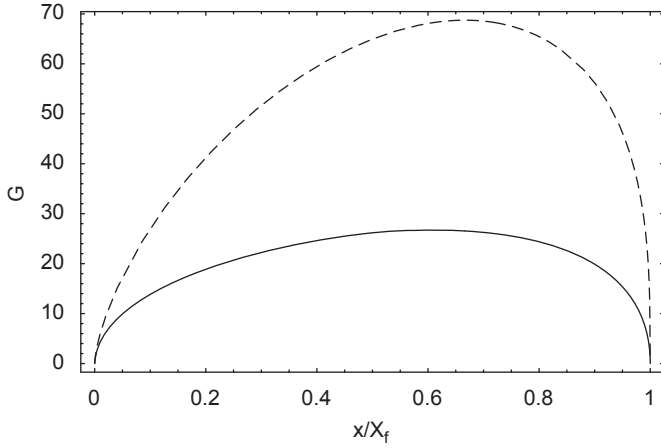


Fig. 2. Comparison of the two-stream instability gain as a function of x/X_f for a beam with velocity tilt (solid curve) and without velocity tilt (dashed curve) for $\delta_0 = (\omega_{pb}^0/\omega_{pe})^2 = 10^{-3}$ and $\alpha^2 = (\omega_{pb}^0 T_f)^2 = 1000$.

with eikonal function S given by

$$S(\bar{\tau}, X, s) = \beta \bar{\tau} s \left[1 \pm i 2 \gamma \int_{\sqrt{1-X}}^1 \frac{dz}{\sqrt{1-s^2 z^4}} \right] \quad (25)$$

where $s = q/(1-X)$ and $\gamma = \alpha \sqrt{1-X}/\beta \bar{\tau}$. For large $|S| \gg 1$, we use the method of stationary phase to calculate S , making use of the smallness of γ in the region $\alpha \sqrt{1-X}/\beta \bar{\tau} = \gamma \ll 1$. The exponentially growing contributions comes from the extremum values of S at $s_{\pm}^0 = \pm(1 + \gamma^2/2)$, and are given by

$$S_{\pm}(s_{\pm}^0) = \beta \bar{\tau} (1 - \gamma^2/2) - iG(X) = \beta \bar{\tau} - \frac{\alpha^2}{2\beta} \left[\frac{1-X}{\tau} \right] + \bar{S}(X). \quad (26)$$

Here the gain function $G(X)$, which determines the amplitude according to $|a| \sim \exp[G(X)]$, is given by Refs. [2,10]

$$G(X) = i\bar{S}(X) = \alpha \sqrt{2(1-X)} F[\text{ArcCos}(\sqrt{1-X})|1/2]. \quad (27)$$

Here, $F(x|\lambda) \equiv \int_0^x d\theta / \sqrt{1 - \lambda \sin^2 \theta}$ is an elliptic integral of the first kind [19]. We conclude from Eq. (27) that the number of e-foldings before linear saturation is determined by the number of beam plasma oscillation periods during the time it takes the beam to compress, which is proportional to $\alpha = \omega_{pb}^0 T_f$. Fig. 2 shows a comparison of the instability gain as a function of x/X_f for an ion beam with velocity tilt (solid curve) and without velocity tilt (dashed curve) for $\delta_0 = (\omega_{pb}^0/\omega_{pe})^2 = 10^{-3}$ and $\alpha^2 = (\omega_{pb}^0 T_f)^2 = 1000$, i.e.,

$$G_{\text{notilt}}(X, t = T_f) = \alpha \frac{3\sqrt{3} X^{2/3} (1-X)^{1/3}}{4 \delta_0^{1/6}}. \quad (28)$$

As evident from the figure, for $\delta_0^{1/6} \ll 1$ the velocity tilt significantly reduces the growth rate compared to the case of a beam with zero initial velocity tilt.

7. Filamentation (Weibel) instability

An intense ion beam propagating through a neutralizing background plasma is also unstable to transverse electromagnetic perturbations. Consider an ion beam propagating in the x -direction through a neutralizing background plasma with velocity $v_{b\parallel}$. Assume that the beam is displaced in the transverse z -direction with a displacement $\delta Z(z)$. For slow processes with characteristic frequency $\omega \ll \omega_{pe}$, the background electrons will neutralize the space-charge produced by the displacement, but the beam current will not be neutralized if the characteristic size of the transverse displacement is less than the skin depth

$\delta_{pe} = c/\omega_{pe}$. As shown below, such a displacement will grow exponentially in time. The density variation due to the displacement $\delta Z(z)$ can be estimated from

$$\delta n = -n_0 \frac{\partial(\delta Z)}{\partial z}. \quad (29)$$

From Ampere's law we obtain

$$-\frac{\partial B}{\partial z} = \frac{4\pi}{c} q v_{b\parallel} \delta n = -\frac{4\pi}{c} q v_{b\parallel} n_0 \frac{\partial(\delta Z)}{\partial z}. \quad (30)$$

The acceleration due to the Lorentz force is given by

$$\frac{d^2(\delta Z)}{dt^2} = \frac{q}{mc} v_{b\parallel} B = \left(\frac{v_{b\parallel}}{c} \right)^2 \left(\frac{4\pi q^2 n_0}{mc} \right) (\delta Z) = \gamma_0^2 (\delta Z). \quad (31)$$

From Eq. (31), we obtain the simple dispersion relation for the Weibel instability

$$\omega = \mathbf{k} \cdot \mathbf{v}_b + i\omega_{pb} \frac{v_{b\parallel}}{c} - i v_{thb} k_{\perp} \quad (32)$$

where \mathbf{v}_b is the directed beam velocity and ω is the complex oscillation frequency. Here, $\gamma_0 = \omega_{pb} v_b/c$ is the characteristic growth rate of the Weibel instability and ω_{pb} is the ion beam plasma frequency. Eq. (32) also includes Landau damping of the perturbation calculated for a Lorentzian transverse velocity distribution with characteristic thermal velocity v_{thb} .

7.1. Ion beam filamentation during transverse compression

For a neutralized ion beam propagating with velocity v_b and converging over a distance X_f , the flow velocity, density, and transverse temperature vary with distance according to Eq. (3). The beam current remains unneutralized at the beam edge over a characteristic transverse distance $\Delta x_{\perp} \sim \delta_{pe}$, where $\delta_{pe} = c/\omega_{pe}$ is the collisionless skin depth. To neglect the beam's pinching contribution to the beam velocity profile in Eq. (3), the condition $R_0 > \alpha \delta_{pe}$ must be satisfied. Here, $\alpha = \omega_{pb} X_f/c > 1$. In what follows, we assume that this condition is satisfied.

By changing variables (x_{\perp}, x) to (y, u) , where $u = 1/(1-x/X_f)$ and $y = x_{\perp} u$, the equation for S can be expressed as

$$-\frac{\partial S}{\partial t} - \frac{u^2 v_b}{X_f} \frac{\partial S}{\partial u} = i\gamma_0 u - i v_{th0} u^2 \frac{\partial S}{\partial y}. \quad (33)$$

Since t and y are cyclic, the *full integral* for S can be expressed as

$$S = -\omega t + k_0 y - \frac{\omega X_f}{v_b} \frac{1}{u} - i \frac{\gamma_0 X_f}{v_b} \ln u + i \frac{v_{th0}}{v_b} k_0 X_f (u-1), \quad (34)$$

where ω and k_0 are constants. The solution for the amplitude in the WKB approximation then becomes

$$a \sim \exp(iS) = \frac{\exp \left[-(k_0 X_f) \left(\frac{v_{th0}}{v_b} \right) \left(\frac{x}{X_f - x} \right) \right]}{(1-x/X_f)^{\alpha}} \times \exp \left[-\omega(t - z/v_b) + i \frac{k_0 x_{\perp}}{1-x/X_f} \right]. \quad (35)$$

Here, $\alpha = \gamma_0 X_f/v_b = \omega_{pb}^0 X_f/c$. Note that the instability has faster than exponential growth. Moreover, the transverse wavenumber increases according to

$$k_{\perp} = \frac{k_0}{(1-x/X_f)}. \quad (36)$$

The maximum of the amplitude is achieved at

$$\frac{1}{u_{\max}} = 1 - \frac{x_{\max}}{X_f} = \frac{k_0 v_{th0}}{\gamma_0} \quad (37)$$

with the maximum number of e-foldings G_{max} given by [8]

$$G_{max} = \alpha \left[\frac{1}{u_{max}} - \ln \frac{e}{u_{max}} \right]. \quad (38)$$

For ballistic focusing, we make use of the solution of the envelope equation

$$R^2(u) = R_f^2 + \frac{1}{u^2} \left(\frac{\varepsilon X_f}{R_f} \right)^2 \quad (39)$$

with constant emittance $\varepsilon = R_0 v_{th0} / v_b$, to relate the initial thermal velocity v_{th0} to the beam radius at the focus by

$$v_{th0} = v_b \frac{R_f}{X_f}. \quad (40)$$

The smallest value of k_0 is given by the $k_0^{min} \sim 1/\delta_{pe}$, and therefore, the maximum of the amplitude is reached at

$$\frac{1}{u_{max}} = 1 - \frac{x_{max}}{X_f} \sim \frac{1}{\alpha} \frac{R_f}{\delta_{pe}} = \frac{R_{max}}{R_0} \quad (41)$$

with maximum number of e-foldings G_{max} given by

$$G_{max} \approx \alpha \ln \left[\alpha \frac{\delta_{pe}}{R_f} \right] = \alpha \ln \left[\frac{R_0}{R_{max}} \right] \quad (42)$$

where the expression in Eq. (42) is evaluated with logarithmic accuracy. Here $R_{max} = R_f(R_0/\alpha\delta_{pe})$ is the beam radius with the largest perturbation amplitude.

It follows from Eq. (42) that to keep the number of e-folding from becoming excessively large, the condition $\alpha \lesssim 1$ must be satisfied [8].

7.2. Weibel instability during longitudinal compression

For a beam compressing longitudinally, with density and velocity changing according to Eqs. (4)–(5), the Hamilton–Jacobi equation for the Weibel instability is given by

$$-\frac{\partial S}{\partial t} = v_b^0 \left(\frac{1-x/X_f}{1-t/T_f} \right) \frac{\partial S}{\partial x} + i \frac{\gamma_0}{(1-t/T_f)^{1/2}}. \quad (43)$$

After the change of variables, $S = S(u, t)$ with $u = (1-t/T_f)/(1-x/X_f)$, the Hamilton–Jacobi equation (43) becomes

$$-\frac{\partial S}{\partial t} = i \frac{\gamma_0}{(1-t/T_f)^{1/2}}. \quad (44)$$

The solution to Eq. (44) satisfying the correct boundary condition $S(x=0, t) = 0$ is given by

$$S = -iG = -iG_0(x)Q(x, t) = -i\alpha \left(\frac{x}{X_f} \right) \times \left\{ \frac{2(1-t/T_f)^{1/2}}{x/X_f} \left[\frac{1}{(1-x/X_f)^{1/2}} - 1 \right] \right\}. \quad (45)$$

Here G is the total gain function, and $G_0(x) = \alpha x/X_f$ is the gain function in the absence of velocity tilt. Also, $x < v_b^0 t$ in Eq. (45).

Introducing the new variable measuring the distance from the head of the beam, $Z = v_b^0 t - x$, the enhancement factor Q can be expressed as

$$Q(Z, x) = \frac{2(1-Z/X_f - x/X_f)^{1/2}}{x/X_f} \times \left[\frac{1}{(1-x/X_f)^{1/2}} - 1 \right]. \quad (46)$$

The largest enhancement is at the head of the beam pulse ($Z = 0$), where

$$Q(Z=0, x) = \frac{2}{x/X_f} [1 - (1-x/X_f)^{1/2}]. \quad (47)$$

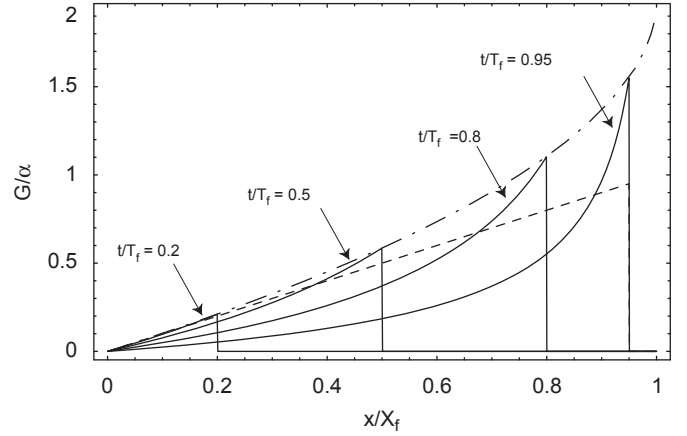


Fig. 3. Normalized gain G/α for the Weibel instability plotted as a function of x/X_f for an intense ion beam with velocity tilt (solid curve) and without velocity tilt (dashed curve), at several instants of time during the compression, $t/T_f = 0.2, 0.5, 0.8, 0.95$. The dashed-dotted curve corresponds to the gain at the head of the pulse ($x = v_b^0 t$).

Note that $Q(Z=0, x)$ increases monotonically from $Q(Z=0, x=0) = 1$ at the beam entrance ($x=0$) to $Q(Z=0, x=X_f) = 2$ at the focal point ($x=X_f$).

The normalized gain function G/α is plotted as function of the normalized spacial variable x/X_f at several instances of time during the compression corresponding to $t/T_f = 0.2, 0.5, 0.8, 0.95$ in Fig. 3. As evident from the figure, for every position along the x -direction, the maximum gain is reached at the head of the pulse, and decreases with time after the head has passed. The largest value of the gain ($G_{max} = 2\alpha$) is achieved at the point of maximum compression ($x = X_f$) at time $t = T_f$.

8. Conclusions

In this paper, the geometrical optics eikonal (WKB) approach to studying the space–time development of beam–plasma instabilities has been summarized in considerable detail. This approach only requires a knowledge of the linear dispersion relation, which plays the role of a first-order partial-differential nonlinear Hamilton–Jacobi equation for the eikonal S . The methods for solving this equation can be adopted from classical mechanics, where a determination of the solution of the Hamilton–Jacobi equation is equivalent to solving the complete orbit mechanics problem. This approach is well suited for studying the instabilities associated with the different types of beam–plasma flows which change in space and time much more slowly than the unstable perturbation. In this case the unstable perturbation can be represented as a sum (integral) over waves, $\exp[iS(t, \mathbf{x}, \mathbf{q})]$, with different local wavenumbers \mathbf{q} . This requires that the waves are almost plane waves locally, or that the WKB approximation holds for each separate wave, i.e., $|S''| \ll |S'|^2$. If the instability is sufficiently well developed that $|S| \gg 1$, the asymptotic space–time development of the instability can be determined by finding stationary points where S has a minimum as function of the parameters \mathbf{q} .

The application of this approach has been illustrated with four examples relevant to ion-beam-driven high energy density physics and heavy ion fusion. In particular, we have studied the electrostatic two-stream and electromagnetic Weibel instabilities for an intense heavy ion beam propagating through a neutralizing background plasma, while the ion beam simultaneously converges transversely and longitudinally. Using this approach we have recovered key stability results with considerably less effort

than that required to solve a linear system of integro-differential equations describing the unstable beam-plasma system.

It has been shown that the two-stream instability for a radially converging beam has a much larger growth rate compared with the case of a non-converging beam [9] [Eq. (18)]. We have also confirmed our previous result [2,10] that longitudinal compression leads to a significant reduction in the growth rate of the two-stream instability compared with the case without an initial velocity tilt. This reduction is by an approximate factor

$$G_{\max}/G_{\max}^{\text{notilt}} \sim (\omega_{pb}/\omega_{pe})^{1/3} \ll 1. \quad (48)$$

This is because longitudinal compression prevents the instability from being driven resonantly by the beam, and the instability saturates linearly, with the number of e-foldings proportional to the number of beam-plasma periods $1/\omega_{pb}$ during the compression time T_f . Therefore, the two-stream instability can be completely mitigated by the effects of longitudinal beam compression when $\omega_{pb}T_f \leq 1$.

The study of the electromagnetic filamentation (Weibel) instability for an intense heavy ion beam radially converging in a background collisionless plasma has demonstrated that a transverse thermal velocity spread limits the number of e-foldings, with maximum growth proportional to $\alpha = \omega_{pb}X_f/c$, where X_f is the compression length [8]. Therefore, to keep the number of e-foldings from being excessively large, the condition $\alpha \leq 1$ must be satisfied. The longitudinal compression also has a large effect on the Weibel instability. The maximum gain in this case is reached at the head of the pulse, and decreases with time after the head has passed the observation point. The largest value of the gain ($G_{\max} = 2\alpha$) is twice as large as that without compression, and is reached at the point of maximum compression ($x = X_f$) at time $t = T_f$ [see Fig. 3].

Acknowledgment

This research was supported by the US Department of Energy.

References

- [1] R.C. Davidson, H. Qin, *Physics of Intense Charged Particle Beams in High Energy Accelerators*, World Scientific, Singapore, 2001, and references therein.
- [2] E.A. Startsev, R.C. Davidson, *Phys. Plasmas* 13 (2006) 062108.
- [3] P.K. Roy, S.S. Yu, et al., *Phys. Rev. Lett.* 95 (2005) 234801.
- [4] D.R. Welch, D.V. Rose, T.C. Genoni, S.S. Yu, J.J. Barnard, *Nucl. Instr. and Meth. A* 544 (2005) 236.
- [5] C. Thoma, D.R. Welch, S.S. Yu, E. Henestroza, P.K. Roy, S. Eylon, E.P. Gilson, *Phys. Plasmas* 12 (2005) 043102.
- [6] P.K. Roy, S.S. Yu, S. Eylon, et al., *Phys. Plasmas* 11 (2004) 2890.
- [7] I. Kaganovich, E.A. Startsev, R.C. Davidson, *Phys. Plasmas* 11 (2004) 3546.
- [8] E.P. Lee, S. Yu, H.L. Buchanan, F.W. Chambers, M.N. Rosenbluth, *Phys. Fluids* 23 (1980) 2095.
- [9] T.C. Genoni, D.V. Rose, D.R. Welch, E.R. Lee, *Phys. Plasmas* 11 (2004) L73.
- [10] E.A. Startsev, R.C. Davidson, *Nucl. Instr. and Meth. A* 577 (2007) 79.
- [11] M. Born, E. Wolf, *Principles of Optics*, Pergamon Press, New York, 1959, p. 109.
- [12] D.D. Ryutov, *Sov. Phys. JETP* 30 (1970) 131.
- [13] I. Haber, in: *Proceedings of the Symposium on Accelerator Aspects of Heavy Ion Fusion*, GSI, Darmstadt, 1982, p. 372.
- [14] I. Hoffmann, I. Bozsik, in: *Proceedings of the Symposium on Accelerator Aspects of Heavy Ion Fusion*, GSI, Darmstadt, 1982, p. 362.
- [15] J. Bisognano, E.P. Lee, J.W.-K. Mark, LLNL Report No. 3-28, 1985.
- [16] C. Jun, H. Qin, R.C. Davidson, P. Heitzenroeder, in: *Proceedings of the 2001 Particle Accelerator Conference*, vol. 3, 2001, p. 1761.
- [17] E.A. Startsev, R.C. Davidson, *New J. Phys.* 6 (2004) 141.
- [18] R. Briggs, in: A. Symon, W.B. Thompson (Eds.), *Advances in Plasma Physics*, vol. 4, Wiley Interscience, New York, 1971, p. 43.
- [19] I.S. Gradshteyn, I.M. Ryzhik, *Table of Integrals, Series, and Products*, Academic Press, New York, London, 1965.